Acta Crystallographica Section F
**Structural Biology and Crystallization Communications**
ISSN 1744-3091

# Crystallization and preliminary X-ray diffraction analysis of Sfh3, a member of the Sec14 protein superfamily

**Jihui Ren,[a]* Gabriel Schaaf,[a] Vytas A. Bankaitis,[a] Eric A. Ortlund[b] and Manish C. Pathak[b]***

[a]Department of Cell and Developmental Biology, Lineberger Comprehensive Cancer Center, University of North Carolina School of Medicine, Chapel Hill, NC 27599-7090, USA, and [b]Department of Biochemistry, Emory University School of Medicine, Atlanta, GA 30322, USA

Correspondence e-mail: jihui_ren@med.unc.edu, mcpatha@emory.edu

Received 14 June 2011
Accepted 6 July 2011

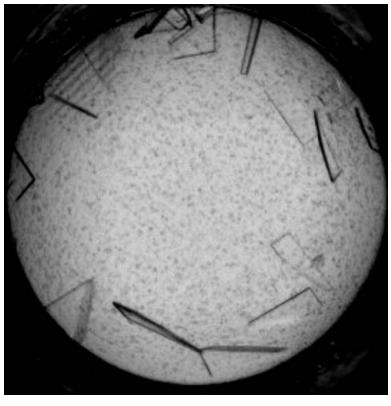



Sec14 is the major phosphatidylinositol (PtdIns)/phosphatidylcholine (PtdCho) transfer protein in the yeast *Saccharomyces cerevisiae* and is the founding member of the Sec14 protein superfamily. Recent functional data suggest that Sec14 functions as a nanoreactor for PtdCho-regulated presentation of PtdIns to PtdIns kinase to affect membrane trafficking. Extrapolation of this concept to other members of the Sec14 superfamily suggests a mechanism by which a comprehensive cohort of Sec14-like nanoreactors sense correspondingly diverse pools of lipid metabolites. In turn, metabolic information is translated to signaling circuits driven by phosphoinositide metabolism. Sfh3, one of five Sec14 homologs in yeast, exhibits several interesting functional features, including its unique localization to lipid particles and microsomes. This localization forecasts novel regulatory interfaces between neutral lipid metabolism and phosphoinositide signaling. To launch a detailed structural and functional characterization of Sfh3, the recombinant protein was purified to homogeneity, diffraction-quality crystals were produced and a native X-ray data set was collected to 2.2 Å resolution. To aid in phasing, SAD X-ray diffraction data were collected to 1.93 Å resolution from an SeMet-labeled crystal at the Southeast Regional Collaborative Access Team at the Advanced Photon Source. Here, the cloning and purification of Sfh3 and the preliminary diffraction of Sfh3 crystals are reported, enabling structural analyses that are expected to reveal novel principles governing ligand binding and functional specificity for Sec14-superfamily proteins.

## 1. Introduction

Membrane trafficking is central to cellular processes in eukaryotic organisms. The *Saccharomyces cerevisiae SEC14* gene product (Sec14) is the founding member of the Sec14 superfamily of proteins, which contains over 500 distinct proteins. It is the major phosphatidylinositol (PtdIns)/phosphatidylcholine (PtdCho) transfer protein in yeast and plays an essential role in stimulating protein transport from the trans-Golgi network (Bankaitis *et al.*, 1990). Sec14 proteins coordinate critical aspects of lipid metabolism with the action of proteins that catalyze the biogenesis of transport vesicles on the trans-Golgi network and endosomal membranes (Cleves *et al.*, 1991; McGee *et al.*, 1994; Xie *et al.*, 1998; Li *et al.*, 2002; Yanagisawa *et al.*, 2002; Bankaitis *et al.*, 2010). Understanding the mechanics of how Sec14-like proteins execute phospholipid (PL) exchange is of central importance given that heterotypic PL-exchange reactions lie at the heart of the mechanisms by which these proteins integrate lipid metabolism with phosphoinositide (PIP) signaling (Schaaf *et al.*, 2008; Bankaitis *et al.*, 2010).

Sfh3 (Sec 14 homolog 3) is only distantly related to Sec14, sharing ~25% identity over essentially the entire primary sequence (Li *et al.*, 2000). Like Sec14, Sfh3 catalyzes PtdIns transfer. However, other biological assays demonstrate that the functional properties of Sfh3 fundamentally differ from those of Sec14 (Li *et al.*, 2000; Routt *et al.*, 2005). While Sfh3 is speculated to play a role in sterol biosynthesis (Griac, 2007), the data to this effect are indirect and weak. Sfh3 localizes to lipid particles and microsomes; however, the function of Sfh3 at these sites remains uncharacterized. The mechanisms which functionally distinguish Sec14 from Sfh3 remain unknown.

To investigate Sfh3 function from a structural perspective, we purified Sfh3 and generated diffraction-quality crystals of both native and SeMet-substituted proteins. Corresponding data sets were collected at 2.2 and 1.93 Å, respectively. Experimental phasing of SeMet-Sfh3 is under way. The Sfh3 structure is expected to reveal new principles regarding the functional engineering of lipid-metabolic nanoreactors of the Sec14 protein superfamily.

## 2. Materials and methods

### 2.1. Cloning and expression of recombinant Sfh3

DNA manipulations were carried out using standard protocols. The entire *SFH3* open-reading frame was amplified from yeast genomic DNA by the polymerase chain reaction using 5′-CGGggtaccATGTTCAAGAGATTTAGCAAAAAG-3′ and 5′-CGGgagctcTTACACGGTACTGCTTTCCG-3′ as the forward and reverse oligonucleotide primers, respectively. The amplified product was adenine-tailed and incorporated into the pGEM-T Easy Vector (Promega, Madison, Wisconsin, USA) following the manufacturer's instructions to generate plasmid pGEM-*SFH3*. To create an expression system for an octahistidine-tagged version of Sfh3 ($His_8$-Sfh3), the *SFH3*-coding region was excised from pGEM-*SFH3* by digestion with *Kpn*I and *Sac*I restriction endonucleases. The purified DNA fragment was subcloned into a modified version of bacterial expression vector PET28b (Novagen, Madison, Wisconsin, USA) in which an octahistidine-tag coding cassette followed by a *Kpn*I site was inserted into the unique *Nco*I site of the vector.

### 2.2. Protein purification and SeMet derivatization

The PET28-*SFH3* construct was transferred into *Escherichia coli* BL21-CodonPlus(DE3)-RIL cells (Stratagene, La Jolla, California, USA). Protein expression was induced by the addition of 100 µ*M* IPTG to the growth medium and cultures were incubated for a further 20 h at 289 K before harvesting cells. Cell-free lysates were generated by lysozyme digestion followed by collisional disruption with glass beads. Crude cell lysates were clarified by serial centrifugation at 26 000*g* and 100 000*g* and the clarified supernatants were incubated with Talon $Co^{2+}$ resin (BD Biosciences Clontech) overnight at 277 K with agitation. The $Co^{2+}$ resin was collected by centrifugation and thoroughly washed with lysis buffer (300 m*M* NaCl, 50 m*M* sodium phosphate pH 7.5, 2 m*M* β-mercaptoethanol) supplemented with 5 m*M* imidazole. Bound proteins were eluted with a linear 5–200 m*M* imidazole gradient and fractions containing $His_8$-Sfh3 were identified by SDS–PAGE and Coomassie staining. Peak fractions were pooled and buffer-exchanged against lysis buffer to remove imidazole. $His_8$-Sfh3 was then concentrated to 8 mg ml$^{-1}$. Typically, we recovered 20 mg soluble $His_8$-Sfh3 from a litre of culture. The $His_8$-Sfh3 protein was subjected to further purification by Sephadex G200 gel-filtration chromatography prior to crystallization trials.

Purification of SeMet-derivatized $His_8$-Sfh3 essentially followed the procedure described above. However, the *E. coli* methionine-auxotrophic strain B834 was used as a production vehicle (Hendrickson *et al.*, 1990). Cells were cultured in medium containing SeMet (Molecular Dimensions, UK) in lieu of methionine to effect substitution.

### 2.3. Crystallization

Initial screening was performed at the Hauptman–Woodward Medical Research Institute high-throughput screening laboratory (Luft *et al.*, 2003). Crystals began appearing after 24 h under a number of conditions and these were subsequently optimized using the sitting-drop vapor-diffusion method in 24-well VDX greased plates (Hampton Research). The reservoir solution consisted of 15–30% PEG 4000, 5% glycerol, 100 m*M* ammonium sulfate, 100 m*M* ammonium acetate pH 5.6. Thin plate-like crystals were harvested 3–4 d after mixing 2 µl protein solution (5 mg ml$^{-1}$) with 2 µl reservoir solution.

### 2.4. X-ray data collection and processing

Sfh3 crystals were transferred to a cryoprotectant solution containing 25%(*v*/*v*) glycerol and flash-cooled in liquid nitrogen prior to diffraction data collection at 100 K on beamline 22-ID at the Southeast Regional Collaborative Access Team (SER-CAT) facility at the Advanced Photon Source (Argonne National Laboratory, Argonne, Illinois, USA). A total of 360 images with an oscillation range of 0.5° were collected from a single crystal at 100 K using a beam size of 50 × 50 µm. A 2.2 Å resolution X-ray diffraction data set was collected from a native Sfh3 crystal and processed in space group $P2_12_12_1$. A selenium single-wavelength anomalous dispersion

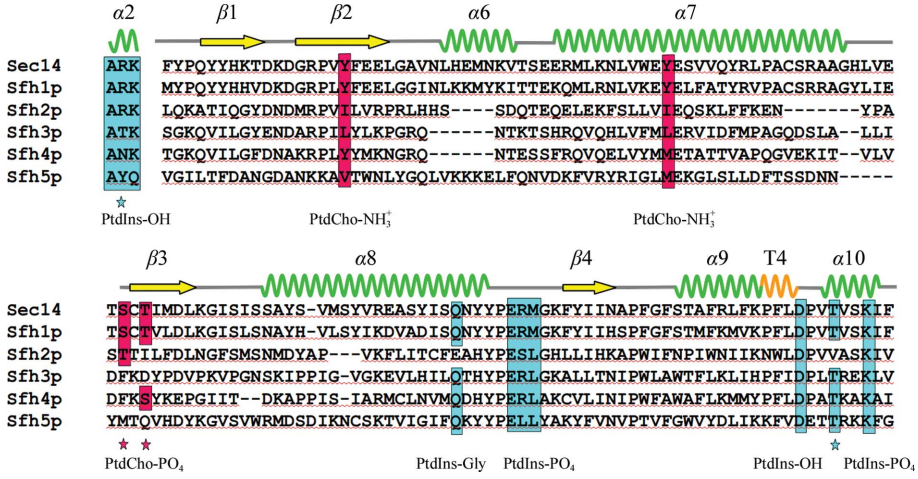


**Figure 1**
Sequence alignment of Sec14-like proteins, with amino-acid residues which interact with PtdCho and PtdIns headgroups in Sfh1 (and Sec14) shaded pink and cyan, respectively. Protein sequences were aligned using *ClustalW*2 (Chenna *et al.*, 2003) on the EBI webserver using the Gonnet protein weight matrix. Gap-open and gap-extension values were set to 10 and 0.1, respectively.

(SAD) data set was also collected to 1.93 Å resolution from an SeMet-derivatized Sfh3 crystal at a wavelength of 0.97820 Å and processed in space group $P2_12_12_1$. Data were indexed, integrated and scaled using *HKL*-2000 (Otwinowski & Minor, 1997). Calculation of the self-rotation function was carried out using the program *MOLREP* (Winn *et al.*, 2011) and structure-factor amplitudes to a maximum resolution of 4.0 Å. The native Patterson synthesis was calculated using the program *FFT* (Winn *et al.*, 2011).

## 3. Results and concluding remarks

*S. cerevisiae* Sec14 is the major yeast phosphatidylinositol (PtdIns)/phosphatidylcholine (PtdCho) transfer protein and is the founding member of the Sec14-protein superfamily. Structural studies revealed that Sec14 binds its two phospholipid ligands (PtdIns and PtdCho) at surprisingly distinct, but overlapping, binding sites (Schaaf *et al.*, 2008). Functional analyses further demonstrated that the capacity to bind both PtdIns and PtdCho must be housed within a single protein molecule in order to produce a biologically active Sec14 protein. These data are interpreted in a PtdIns presentation model in which Sec14 functions as a nanoreactor for PtdCho-regulated presentation of PtdIns to PtdIns kinase. In this way, the Sec14 nanoreactor senses PtdCho metabolism and translates it to phosphoinositide phosphate (PIP) synthesis to regulate specific membrane-trafficking pathways. Structure-based bioinformatics methods predict that the PtdIns-binding site is conserved in the Sec14 superfamily, while the PtdCho-binding site is missing from most of the Sec14-like proteins (Fig. 1). While Sfh3 maintains the PtdIns-binding motif, it does not exhibit a recognizable PtdCho-binding motif (Fig. 1). Specifically, Sec14 and its closely related homolog Sfh1 utilize Tyr residues to stabilize the positively charged PtdCho headgroup *via* cation–$\pi$ interactions (Schaaf *et al.*, 2008). Sfh3 contains Leu residues at these positions. These substitutions, while not formally incompatible with PtdCho coordination, are not predicted to favor burial of the choline moiety deep within the hydrophobic protein core. The low sequence identity that Sfh3 shares with Sec14, when coupled with its predicted lack of PtdCho-binding ability, forecasts that Sfh3 will exhibit novel structural and functional features. Indeed, while Sfh3 is expected to display the overall Sec14 (or CRAL-TRIO) architecture observed in members of the Sec14 family of proteins, considerable structural variation is observed across family members in the 'gating helix' which controls access to the phospholipid-binding pocket (Phillips *et al.*, 1999; Sha *et al.*, 1998; Schaaf *et al.*, 2008; Min *et al.*, 2003; Meier *et al.*, 2003; Stocker & Baumann, 2003; D'Angelo *et al.*, 2006; Welti *et al.*, 2007). Given its distinct cellular localization, it is possible that Sfh3 recognizes lipids beyond PtdIns. The identification of the second lipid ligand other than PtdIns is pivotal to understanding the biological function of proteins in the Sec14 superfamily. Crystallographic studies are a critical first step towards the characterization of novel lipid–Sfh3 interactions and the molecular mechanisms driving lipid binding and exchange.

Sfh3 was purified to homogeneity by means of $Co^{2+}$-affinity and size-exclusion chromatography (Fig. 2). Crystallization proceeded rapidly and thin plate-like crystals were harvested after 3–4 d (Fig. 3).

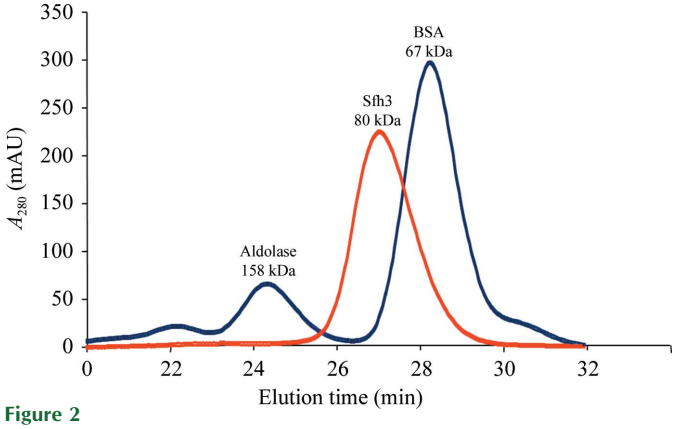


**Figure 2**
Gel-filtration chromatogram of purified recombinant Sfh3 fractionated by Sephadex G-200 size-exclusion chromatography. Elution profiles of the protein markers BSA (67 kDa) and aldolase (158 kDa) are shown. Sfh3 (80 kDa) filters at a position consistent with a dimer.

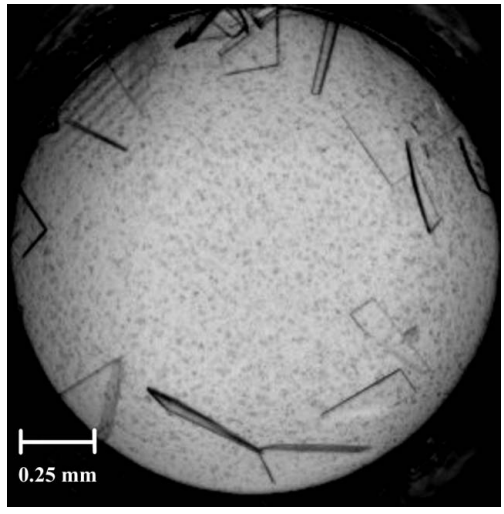


**Figure 3**
Three-dimensional plate-like crystals of Sfh3 grew from 15–30% PEG 4000, 5% glycerol, 100 m*M* ammonium sulfate, 100 m*M* ammonium acetate pH 5.6.

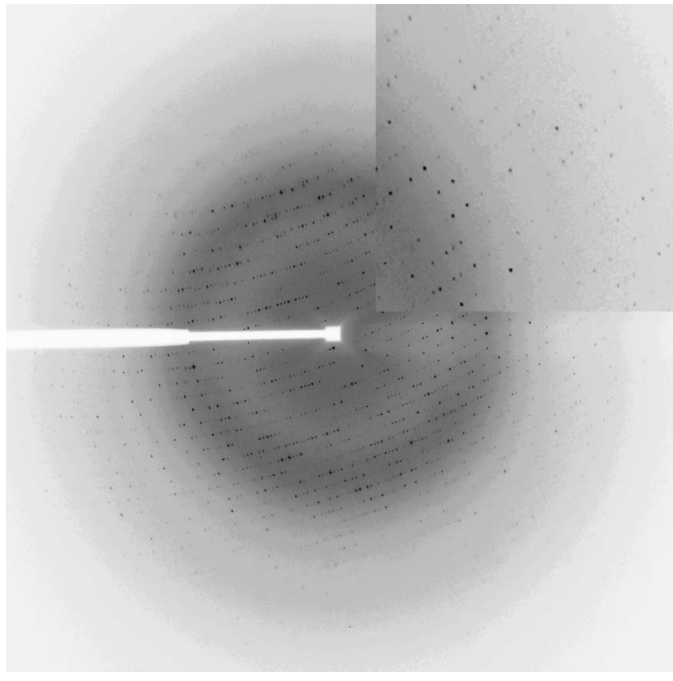

**Figure 4**
X-ray diffraction image from a native Sfh3 crystal (0.5° oscillation) collected on SER-CAT beamline 22-ID using a MAR CCD 300 detector at a wavelength of 1.0 Å. Diffraction extends to the detector edge, which corresponds to a resolution of 1.85 Å.

Despite their non-ideal morphology, diffraction data were collected to 2.2 Å resolution from these crystals. The X-ray diffraction data set was processed in space group $P2_12_12_1$, with unit-cell parameters $a$ = 52.65, $b$ = 112.03, $c$ = 144.91 Å (Fig. 4, Table 1). Systematic absences for odd reflections in the cases of $h00$, $0k0$ and $00l$ indicated the presence of a $2_1$ screw axis along all three axes. A self-rotation function (Rossmann & Blow, 1962) calculated using 4 Å resolution data in the $\kappa$ = 180° section showed strong pseudo-translation together with peaks that correspond to three mutually orthogonal twofold axes, suggesting that the asymmetric unit contains 222 point-group symmetry (Fig. 5). However, no dominant features could be assigned to noncrystallographic axes in the $\kappa$ = 180° section. The observed heights of 3.75$\sigma$ and 3.31$\sigma$ for the corresponding self-rotation peaks are much weaker than the height of 15.47$\sigma$ for the origin peak and exceed the heights of all other peaks by less than twofold. A Patterson function (Patterson, 1935) calculated using all data showed a strong peak at 0.50, 0.50, 0.37, suggesting a dimer (Fig. 6) in the asymmetric unit. The Matthews coefficient is 5.25 Å$^3$ Da$^{-1}$ for one monomer in the asymmetric unit and 2.62 Å$^3$ Da$^{-1}$ for two copies in the asymmetric unit, with solvent contents of 76.6 and 53.2%, respectively. Gel-filtration and hydrodynamic analyses demonstrate that recombinant Sfh3 purifies as a dimer (Fig. 2), suggesting that the asymmetric unit contains one copy of the biologically relevant dimer.

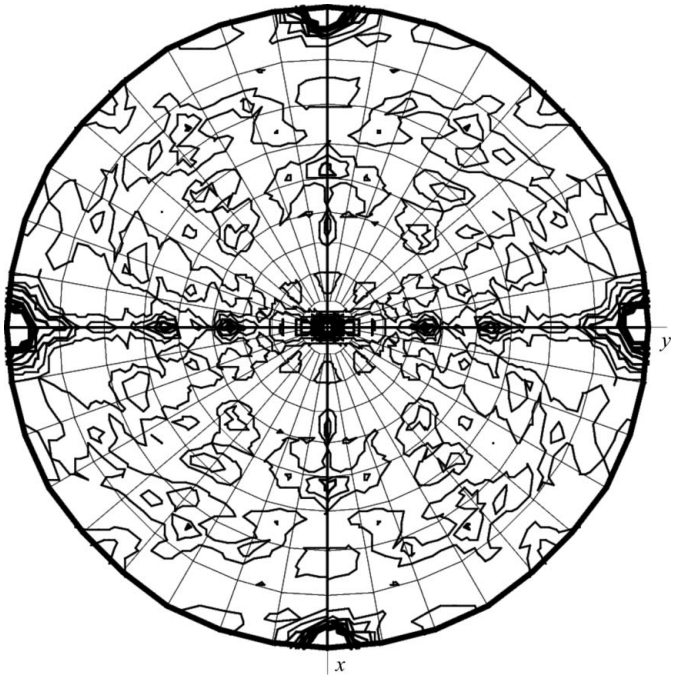


**Figure 5**
Self-rotation function for native Sfh3 in the $\kappa$ = 180° section calculated with *MOLREP* from *CCP*4 (Winn *et al.*, 2011) using default parameters, with a radius of integration of 26.33° and data in the resolution range 39.8 > $d$ > 4.0 Å.

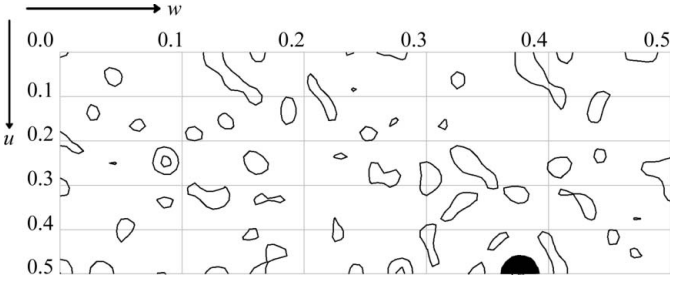


**Figure 6**
Harker section ($u$, $\frac{1}{2}v$, $w$) of the native Patterson map calculated using all data. The large peak located at ($u$, $w$) = (0, 0.3763) corresponds to the translation vector between corresponding atoms in the subunits of the dimer in the asymmetric unit, the noncrystallographic twofold axis of which is parallel to the crystallographic twofold screw axis. The map is contoured from 1.0$\sigma$ in steps of 1.0$\sigma$.

**Table 1**
Native and SeMet-derivatized Sfh3 crystal data-collection statistics.

Values in parentheses are for the highest resolution shell.

| | Native | SeMet |
|---|---|---|
| Wavelength (Å) | 1.00 | 0.97820 |
| Resolution (Å) | 2.20 (2.28–2.20) | 1.93 (2.00–1.93) |
| Space group | $P2_12_12_1$ | $P2_12_12_1$ |
| Unit-cell parameters (Å) | $a$ = 52.65, $b$ = 112.03, $c$ = 144.91 | $a$ = 52.52, $b$ = 114.71, $c$ = 144.69 |
| Unit-cell volume (Å$^3$) | 854772.2 | 871779.4 |
| Total No. of reflections | 316005 | 338750 |
| No. of unique reflections | 43893 | 66699 |
| $R_{\rm merge}$† (%) | 12.1 (68.8) | 7.3 (28.3) |
| Completeness (%) | 100 (100) | 99.9 (99.9) |
| Average multiplicity | 7.2 (6.9) | 5.1 (5.0) |
| $\langle I/\sigma(I)\rangle$ | 28.0 (3.2) | 28.9 (6.0) |
| Molecules per asymmetric unit | 2 | 2 |
| Matthews coefficient (Å$^3$ Da$^{-1}$) | 2.62 | 2.68 |
| Solvent content (%) | 53.16 | 54.07 |
| Mosaicity (°) | 0.89 | 0.46 |

† $R_{\rm merge} = \sum_{hkl}\sum_i |I_i(hkl) - \langle I(hkl)\rangle| / \sum_{hkl}\sum_i I_i(hkl)$, where $I_i(hkl)$ is the observed intensity and $\langle I(hkl)\rangle$ is the average intensity of symmetry-related observations.

Our efforts to phase the native Sfh3 data set by molecular replacement failed using either the 'open' conformation of Sec14 (PDB entry 1aua; Sha *et al.*, 1998) or the 'closed' conformation of Sfh1 (PDB entries 3b74, 3b7n, 3b7q and 3b7z; Schaaf *et al.*, 2008) as search models. Thus, we expect that the conformation of Sfh3 is sufficiently different from previously observed Sec14 structures to prohibit molecular replacement. This intriguing possibility suggests that solution of the Sfh3 structure will capture yet another functionally important conformation for this class of PITPs.

To obtain experimental phase information, recombinant SeMet-derivatized Sfh3 was purified from *E. coli*. Crystals were successfully generated and diffracted to 1.93 Å resolution. A SAD data set was collected to 1.93 Å resolution and processed in space group $P2_12_12_1$, with unit-cell parameters $a$ = 52.52, $b$ = 114.72, $c$ = 144.69 Å (Fig. 4, Table 1). The experimental phasing of Sfh3 is under way and we expect that the forthcoming Sfh3 structure will reveal architectural features that are unique to Sfh3. Such high-resolution information will significantly extend our current understanding of the role of Sec14-like proteins in lipid signaling.

This work was supported by grant GM44530 to VAB from the National Institutes of Health. EAO was supported by start-up funds from Emory University School of Medicine.

## References

Bankaitis, V. A., Aitken, J. R., Cleves, A. E. & Dowhan, W. (1990). *Nature (London)*, **347**, 561–562.
Bankaitis, V. A., Mousley, C. J. & Schaaf, G. (2010). *Trends Biochem. Sci.* **35**, 150–160.
Chenna, R., Sugawara, H., Koike, T., Lopez, R., Gibson, T. J., Higgins, D. G. & Thompson, J. D. (2003). *Nucleic Acids Res.* **31**, 3497–3500.
Cleves, A. E., McGee, T. P., Whitters, E. A., Champion, K. M., Aitken, J. R., Dowhan, W., Goebl, M. & Bankaitis, V. A. (1991). *Cell*, **64**, 789–800.
D'Angelo, I., Welti, S., Bonneau, F. & Scheffzek, K. (2006). *EMBO Rep.* **7**, 174–179.
Griac, P. (2007). *Biochim. Biophys. Acta*, **1771**, 737–745.

Hendrickson, W. A., Horton, J. R. & LeMaster, D. M. (1990). *EMBO J.* **9**, 1665–1672.
Li, X., Rivas, M. P., Fang, M., Marchena, J., Mehrotra, B., Chaudhary, A., Feng, L., Prestwich, G. D. & Bankaitis, V. A. (2002). *J. Cell Biol.* **157**, 63–77.
Li, X., Routt, S. M., Xie, Z., Cui, X., Fang, M., Kearns, M. A., Bard, M., Kirsch, D. R. & Bankaitis, V. A. (2000). *Mol. Biol. Cell*, **11**, 1989–2005.
Luft, J. R., Collins, R. J., Fehrman, N. A., Lauricella, A. M., Veatch, C. K. & DeTitta, G. T. (2003). *J. Struct. Biol.* **142**, 170–179.
McGee, T. P., Skinner, H. B., Whitters, E. A., Henry, S. A. & Bankaitis, V. A. (1994). *J. Cell Biol.* **124**, 273–287.
Meier, R., Tomizaki, T., Schulze-Briese, C., Baumann, U. & Stocker, A. (2003). *J. Mol. Biol.* **331**, 725–734.
Min, K. C., Kovall, R. A. & Hendrickson, W. A. (2003). *Proc. Natl Acad. Sci. USA*, **100**, 14713–14718.
Otwinowski, Z. & Minor, W. (1997). *Methods Enzymol.* **276**, 307–326.
Patterson, A. L. (1935). *Z. Kristallogr.* **90**, 517–542.
Phillips, S. E., Sha, B., Topalof, L., Xie, Z., Alb, J. G., Klenchin, V. A., Swigart, P., Cockcroft, S., Martin, T. F., Luo, M. & Bankaitis, V. A. (1999). *Mol. Cell*, **4**, 187–197.
Rossmann, M. G. & Blow, D. M. (1962). *Acta Cryst.* **15**, 24–31.
Routt, S. M., Ryan, M. M., Tyeryar, K., Rizzieri, K. E., Mousley, C., Roumanie, O., Brennwald, P. J. & Bankaitis, V. A. (2005). *Traffic*, **6**, 1157–1172.
Schaaf, G., Ortlund, E. A., Tyeryar, K. R., Mousley, C. J., Ile, K. E., Garrett, T. A., Ren, J., Woolls, M. J., Raetz, C. R., Redinbo, M. R. & Bankaitis, V. A. (2008). *Mol. Cell*, **29**, 191–206.
Sha, B., Phillips, S. E., Bankaitis, V. A. & Luo, M. (1998). *Nature (London)*, **391**, 506–510.
Stocker, A. & Baumann, U. (2003). *J. Mol. Biol.* **332**, 759–765.
Welti, S., Fraterman, S., D'Angelo, I., Wilm, M. & Scheffzek, K. (2007). *J. Mol. Biol.* **366**, 551–562.
Winn, M. D. *et al.* (2011). *Acta Cryst.* D**67**, 235–242.
Xie, Z., Fang, M., Rivas, M. P., Faulkner, A. J., Sternweis, P. C., Engebrecht, J. A. & Bankaitis, V. A. (1998). *Proc. Natl Acad. Sci. USA*, **95**, 12346–12351.
Yanagisawa, L. L., Marchena, J., Xie, Z., Li, X., Poon, P. P., Singer, R. A., Johnston, G. C., Randazzo, P. A. & Bankaitis, V. A. (2002). *Mol. Biol. Cell*, **13**, 2193–2206.